

# Algebraic entropy fixes and convex limiting for continuous finite element discretizations of scalar hyperbolic conservation laws

Dmitri Kuzmin<sup>a,\*</sup>, Manuel Quezada de Luna<sup>b</sup>

<sup>a</sup>*Institute of Applied Mathematics (LS III), TU Dortmund University  
Vogelpothsweg 87, D-44227 Dortmund, Germany*

<sup>b</sup>*King Abdullah University of Science and Technology (KAUST)  
Thuwal 23955-6900, Saudi Arabia*

---

## Abstract

In this work, we modify a continuous Galerkin discretization of a scalar hyperbolic conservation law using new algebraic correction procedures. Discrete entropy conditions are used to determine the minimal amount of entropy stabilization and constrain antidiffusive corrections of a property-preserving low-order scheme. The addition of a second-order entropy dissipative component to the antidiffusive part of a nearly entropy conservative numerical flux is generally insufficient to prevent violations of local bounds in shock regions. Our monolithic convex limiting technique adjusts a given target flux in a manner which guarantees preservation of invariant domains, validity of local maximum principles, and entropy stability. The new methodology combines the advantages of modern entropy stable / entropy conservative schemes and their local extremum diminishing counterparts. The process of algebraic flux correction is based on inequality constraints which provably provide the desired properties. No free parameters are involved. The proposed algebraic fixes are readily applicable to unstructured meshes, finite element methods, general time discretizations, and steady-state residuals. Numerical studies of explicit entropy-constrained schemes are performed for linear and nonlinear test problems.

*Keywords:* hyperbolic conservation laws, entropy stability, invariant domain preservation, finite elements, algebraic flux correction, convex limiting

---

## 1. Introduction

Entropy stability [8, 29, 33, 34] and preservation of invariant domains [14, 16, 19] play an important role in the design of numerical methods for nonlinear hyperbolic conservation laws. A failure to comply with these design criteria may result in nonphysical artefacts and/or convergence to wrong weak solutions. Modern high-resolution schemes are commonly equipped with flux or slope limiters

---

\*Corresponding author

*Email addresses:* kuzmin@math.uni-dortmund.de (Dmitri Kuzmin), manuel.quezada@kaust.edu.sa (Manuel Quezada de Luna)

which guarantee the validity of discrete maximum principles but may fail to satisfy entropy conditions. On the other hand, entropy stability of a high-order method does not guarantee the invariant domain preservation (IDP) property and numerical solutions may exhibit undershoots/overshoots.

Recent years have witnessed an increased interest of the finite element community in analysis and design of algebraic flux correction (AFC) schemes [5, 6, 20, 21]. The AFC methodology modifies a standard Galerkin discretization by adding artificial diffusion operators and limited antidiffusive fluxes. The convex limiting techniques proposed in [14, 19, 22] are applicable to nonlinear hyperbolic problems and lead to high-order IDP approximations. However, additional inequality constraints must be taken into account to ensure entropy stability. In the context of finite volume and discontinuous Galerkin (DG) approximations, entropy stability is commonly achieved by adding some entropy viscosity to an entropy conservative numerical flux. For a comprehensive review of entropy stable schemes based on this design philosophy, we refer to Tadmor [33, 34]. A representation of continuous finite element approximations in terms of numerical fluxes is also possible [30, 31] but rather uncommon and requires the use of edge-based data structures [25]. Therefore, the use of formulations that add diffusive fluxes to the residual of the Galerkin discretization is preferred in the AFC literature [20].

As shown by Guermond et al. [15], entropy stability is an essential requirement for convergence of AFC schemes to correct weak solutions of nonlinear hyperbolic problems. Residual-based entropy viscosity [14, 15] was found to be a good way to stabilize flux-corrected continuous Galerkin (CG) approximations [14, 22]. However, it involves a free parameter and does not guarantee entropy stability. The entropy fixes proposed by Abgrall et al. [1, 2] use Rusanov-type dissipation terms to enforce a cell entropy inequality. In contrast to finite volume and DG methods, construction of entropy conservative CG schemes for which this inequality holds as equality is an open problem. Hence, the minimal amount of entropy stabilization needs to be determined without enforcing local entropy conservation. The entropy stability conditions that we use in the present paper are derived by adapting Tadmor's [33] design criteria to the CG setting. The key ingredients of the proposed methodology are

- inequality constraints that guarantee entropy stability and preservation of invariant domains;
- a general framework for designing algebraic flux correction schemes based on such constraints;
- new parameter-free algorithms for construction and limiting of entropy stabilization terms.

We begin with the CG space discretization of the initial value problem in Section 2. After introducing the new AFC tools and their theoretical foundations in Sections 3-5, we summarize the proposed algorithm in Section 6, perform numerical studies in Section 7, and draw conclusions in Section 8.

## 2. Finite element discretization

Let  $u(\mathbf{x}, t)$  be a scalar conserved quantity depending on the space location  $\mathbf{x} \in \mathbb{R}^d$ ,  $d \in \{1, 2, 3\}$  and time instant  $t \geq 0$ . Consider an initial value problem of the form

$$\frac{\partial u}{\partial t} + \nabla \cdot \mathbf{f}(u) = 0 \quad \text{in } \mathbb{R}^d \times \mathbb{R}_+, \quad (1a)$$

$$u(\cdot, 0) = u_0 \quad \text{in } \mathbb{R}^d, \quad (1b)$$

where  $\mathbf{f} = (f_1, \dots, f_d)$  is a possibly nonlinear flux function and  $u_0 : \mathbb{R}^d \rightarrow \mathcal{G}$  is an initial data belonging to a convex set  $\mathcal{G}$ . The set  $\mathcal{G}$  is called an *invariant set* of problem (1a)–(1b) if the exact solution  $u$  stays in  $\mathcal{G}$  for all  $t > 0$  [16]. A convex function  $\eta : \mathcal{G} \rightarrow \mathbb{R}$  is called an *entropy* and  $v = \eta'$  is called an *entropy variable* if there exists an *entropy flux*  $\mathbf{q} : \mathcal{G} \rightarrow \mathbb{R}^d$  such that  $v(u)\mathbf{f}'(u) = \mathbf{q}'(u)$ . A weak solution  $u$  of (1a) is called an *entropy solution* if the entropy inequality

$$\frac{\partial \eta}{\partial t} + \nabla \cdot \mathbf{q}(u) \leq 0 \quad \text{in } \mathbb{R}^d \times \mathbb{R}_+ \quad (2)$$

holds for any *entropy pair*  $(\eta, \mathbf{q})$ . For any smooth weak solution, the conservation law

$$\frac{\partial \eta}{\partial t} + \nabla \cdot \mathbf{q}(u) = 0 \quad \text{in } \mathbb{R}^d \times \mathbb{R}_+ \quad (3)$$

can be derived from (1a) using multiplication by the entropy variable  $v$ , the chain rule, and the definition of an entropy pair. Hence, entropy is conserved in smooth regions and dissipated at shocks.

Adopting the terminology of Guermond et al. [14, 16], we will call a numerical scheme *invariant domain preserving* (IDP) if the solution of the (semi-)discrete problem is guaranteed to stay in an invariant set  $\mathcal{G}$ . Additionally, a property-preserving discretization of (1a) should be *entropy stable*, i.e., it should satisfy a discrete version of the entropy inequality (2). The lack of entropy stability is a typical reason for convergence of numerical schemes to nonphysical weak solutions.

Restricting the spatial domain to  $\Omega \subset \mathbb{R}^d$  and imposing periodic boundary conditions for simplicity, we discretize (1a) in space using a conforming mesh  $\mathcal{T}_h = \{K_1, \dots, K_{N_h}\}$  of linear ( $\mathbb{P}_1$ ) or multilinear ( $\mathbb{Q}_1$ ) finite elements. The globally continuous basis functions  $\varphi_1, \dots, \varphi_{N_h}$  are associated with the vertices  $\mathbf{x}_1, \dots, \mathbf{x}_{N_h}$  of  $\mathcal{T}_h$ . Let  $\mathcal{E}_i$  denote the set of (numbers of) elements containing the vertex  $\mathbf{x}_i$  and  $\mathcal{N}^e$  is the set of (numbers of) nodes belonging to  $K^e$ . The computational stencil of node  $i$  is the integer set  $\mathcal{N}_i = \bigcup_{e \in \mathcal{E}_i} \mathcal{N}^e$ . Substituting the finite element approximations

$$u_h = \sum_{j=1}^{N_h} u_j \varphi_j, \quad \mathbf{f}_h = \sum_{j=1}^{N_h} \mathbf{f}_j \varphi_j \approx \mathbf{f}(u_h) \quad (4)$$

into the weak form of (1a) and using  $\varphi_i$ ,  $i \in \{1, \dots, N_h\}$  as a test function, we obtain [19]

$$\sum_{e \in \mathcal{E}_i} \sum_{j \in \mathcal{N}^e} m_{ij}^e \frac{du_j}{dt} = - \sum_{e \in \mathcal{E}_i} \sum_{j \in \mathcal{N}^e} \mathbf{c}_{ij}^e \cdot \mathbf{f}_j = - \sum_{e \in \mathcal{E}_i} \sum_{j \in \mathcal{N}^e \setminus \{i\}} \mathbf{c}_{ij}^e \cdot (\mathbf{f}_j - \mathbf{f}_i), \quad (5)$$

$$m_{ij}^e = \int_{K^e} \varphi_i \varphi_j \, d\mathbf{x}, \quad \mathbf{c}_{ij}^e = \int_{K^e} \varphi_i \nabla \varphi_j \, d\mathbf{x}, \quad \sum_{j \in \mathcal{N}^e} \varphi_j(\mathbf{x}) = 1 \quad \forall \mathbf{x} \in K^e. \quad (6)$$

The choice of the time integration method should ensure at least conditional  $L^2$  stability of the fully discrete problem for linear flux functions of the form  $\mathbf{f}(u) = \mathbf{v}u$ ,  $\mathbf{v} \in \mathbb{R}^d$ . The lack of nonlinear stability can be cured using the algebraic flux correction tools that we present in the next sections.

### 3. Property-preserving flux correction

To enforce entropy inequalities and local discrete maximum principles, we approximate (5) by

$$\sum_{e \in \mathcal{E}_i} m_i^e \frac{du_i}{dt} = \sum_{e \in \mathcal{E}_i} \sum_{j \in \mathcal{N}^e \setminus \{i\}} [g_{ij}^e - \mathbf{c}_{ij}^e \cdot (\mathbf{f}_j - \mathbf{f}_i)], \quad (7)$$

where

$$m_i^e = \sum_{j \in \mathcal{N}^e} m_{ij}^e = \int_{K^e} \varphi_i \, d\mathbf{x} \quad (8)$$

are the diagonal entries of the lumped element mass matrix and  $g_{ij}^e$  are numerical fluxes such that

$$g_{ji}^e = -g_{ij}^e \quad \forall i \in \mathcal{N}^e, j \in \mathcal{N}^e \setminus \{i\}. \quad (9)$$

The standard continuous Galerkin scheme (5) can be written in the form (7) using the fluxes

$$g_{ij}^{e, \text{CG}} = m_{ij}^e (\dot{u}_i - \dot{u}_j). \quad (10)$$

The nodal time derivatives  $\dot{u}_i = \frac{du_i}{dt}$  are defined by (5). To avoid inversion of the consistent mass matrix, an approximate solution of this linear system for  $\dot{u}$  can be obtained efficiently using a few Richardson's iterations preconditioned by the lumped mass matrix [10, 26]. This approach to calculating  $\dot{u}$  corresponds to an approximation by a truncated Neumann series [15, 26].

The purpose of algebraic flux correction (AFC) is to replace  $g_{ij}^{e, \text{CG}}$  with a flux that contains enough numerical dissipation to ensure preservation of invariant domains, validity of local discrete maximum principles and/or entropy stability. On the other hand, the levels of numerical diffusion should be kept small enough to achieve optimal convergence behavior for problems with smooth exact solutions. Similarly to PDE-constrained optimization problems, AFC schemes are designed to adjust the *control variables*  $g_{ij}^e$  in a way which guarantees the validity of certain constraints for the *state variables*  $u_i$  while staying as close as possible to a given *target*. Numerical solution of global constrained optimization problems is feasible [7] but costly. Therefore, we will design  $g_{ij}^e$  using sufficient conditions (box constraints) to derive simple closed-form approximations which provide the desired properties.

Let  $(\eta, \mathbf{q})$  be an entropy pair and  $v = \eta'(u)$  the corresponding entropy variable. Define

$$\boldsymbol{\psi}(u) = v(u)\mathbf{f}(u) - \mathbf{q}(u). \quad (11)$$

A sufficient condition for entropy stability of the semi-discrete problem (7) is given by (cf. [8, 27])

$$\frac{v_i - v_j}{2} [g_{ij}^e - \mathbf{c}_{ij}^e \cdot (\mathbf{f}_j + \mathbf{f}_i)] \leq \mathbf{c}_{ij}^e \cdot [\boldsymbol{\psi}(u_j) - \boldsymbol{\psi}(u_i)]. \quad (12)$$

In the following Theorem, we show that (12) implies the validity of a semi-discrete entropy inequality.

**Theorem 1** (Entropy stability of AFC schemes [14, 16]). *If condition (12) holds for each flux  $g_{ij}^e$ , then the solution of the semi-discrete problem (7) satisfies the discrete entropy inequality*

$$\sum_{e \in \mathcal{E}_i} m_i^e \frac{d\eta(u_i)}{dt} \leq \sum_{e \in \mathcal{E}_i} \sum_{j \in \mathcal{N}^e \setminus \{i\}} [G_{ij}^e - \mathbf{c}_{ij}^e \cdot (\mathbf{q}_j - \mathbf{q}_i)], \quad (13)$$

where

$$G_{ij}^e = \frac{v_i + v_j}{2} g_{ij}^e - \frac{v_i - v_j}{2} \mathbf{c}_{ij}^e \cdot (\mathbf{f}_j - \mathbf{f}_i). \quad (14)$$

PROOF. We have  $\sum_{e \in \mathcal{E}_i} m_i^e \frac{d\eta(u_i)}{dt} = \sum_{e \in \mathcal{E}_i} m_i^e v_i \frac{du_i}{dt} = \sum_{e \in \mathcal{E}_i} v_i \sum_{j \in \mathcal{N}^e \setminus \{i\}} [g_{ij}^e - \mathbf{c}_{ij}^e \cdot (\mathbf{f}_j - \mathbf{f}_i)]$  by the chain rule and the definition of the entropy variable  $v_i = \eta'(u_i)$ . Using the zero sum property  $\sum_{j \in \mathcal{N}^e} \mathbf{c}_{ij}^e = \mathbf{0}$  of the discrete gradient operator, and the stability condition (12), we find that

$$\begin{aligned} & v_i \sum_{j \in \mathcal{N}^e \setminus \{i\}} [g_{ij}^e - \mathbf{c}_{ij}^e \cdot (\mathbf{f}_j - \mathbf{f}_i)] = v_i \sum_{j \in \mathcal{N}^e \setminus \{i\}} [g_{ij}^e - \mathbf{c}_{ij}^e \cdot (\mathbf{f}_j + \mathbf{f}_i)] - 2v_i \mathbf{c}_{ii}^e \cdot \mathbf{f}_i \\ &= \sum_{j \in \mathcal{N}^e \setminus \{i\}} \left( \frac{v_i + v_j}{2} [g_{ij}^e - \mathbf{c}_{ij}^e \cdot (\mathbf{f}_j + \mathbf{f}_i)] + \frac{v_i - v_j}{2} [g_{ij}^e - \mathbf{c}_{ij}^e \cdot (\mathbf{f}_j + \mathbf{f}_i)] \right) - 2v_i \mathbf{c}_{ii}^e \cdot \mathbf{f}_i \\ &\leq \sum_{j \in \mathcal{N}^e \setminus \{i\}} \left( \frac{v_i + v_j}{2} [g_{ij}^e - \mathbf{c}_{ij}^e \cdot (\mathbf{f}_j + \mathbf{f}_i)] + \mathbf{c}_{ij}^e \cdot [\psi(u_j) - \psi(u_i)] \right) - 2v_i \mathbf{c}_{ii}^e \cdot \mathbf{f}_i \\ &= \sum_{j \in \mathcal{N}^e \setminus \{i\}} \left( \frac{v_i + v_j}{2} [g_{ij}^e - \mathbf{c}_{ij}^e \cdot (\mathbf{f}_j + \mathbf{f}_i)] + \mathbf{c}_{ij}^e \cdot [\psi(u_j) + \psi(u_i)] \right) - 2\mathbf{c}_{ii}^e \cdot [v_i \mathbf{f}_i - \psi(u_i)] \\ (*) &= \sum_{j \in \mathcal{N}^e \setminus \{i\}} \left( \frac{v_i + v_j}{2} g_{ij}^e - \mathbf{c}_{ij}^e \cdot \left[ \frac{v_i - v_j}{2} (\mathbf{f}_j - \mathbf{f}_i) + \mathbf{q}_j + \mathbf{q}_i \right] \right) - 2\mathbf{c}_{ii}^e \cdot \mathbf{q}_i \\ &= \sum_{j \in \mathcal{N}^e \setminus \{i\}} \left( \frac{v_i + v_j}{2} g_{ij}^e - \mathbf{c}_{ij}^e \cdot \left[ \frac{v_i - v_j}{2} (\mathbf{f}_j - \mathbf{f}_i) + \mathbf{q}_j - \mathbf{q}_i \right] \right) = \sum_{j \in \mathcal{N}^e \setminus \{i\}} [G_{ij}^e - \mathbf{c}_{ij}^e \cdot (\mathbf{q}_j - \mathbf{q}_i)]. \end{aligned}$$

Summing over  $e \in \mathcal{E}_i$ , we conclude that the assertion of the Theorem is true.  $\square$

By definition of  $\mathbf{c}_{ij}^e$ , we have  $\sum_{e \in \mathcal{E}_i} \mathbf{c}_{ij}^e = -\sum_{e \in \mathcal{E}_i} \mathbf{c}_{ji}^e$  if  $i$  or  $j$  is an interior node. Under the assumption of periodic boundary conditions, this property holds for all nodes. In particular, we have  $\sum_{e \in \mathcal{E}_i} \mathbf{c}_{ii}^e = \mathbf{0}$ . Using the identity marked by (\*) in the proof of Theorem 2, we obtain the estimate

$$\begin{aligned} \sum_{i=1}^{N_h} \sum_{e \in \mathcal{E}_i} m_i^e \frac{d\eta_i}{dt} &\leq \sum_{i=1}^{N_h} \sum_{\substack{j=1 \\ j>i}}^{N_h} \frac{v_i + v_j}{2} \sum_{e \in \mathcal{E}_i} \underbrace{(g_{ij}^e + g_{ji}^e)}_{=0} \\ &\quad - \sum_{i=1}^{N_h} \sum_{\substack{j=1 \\ j>i}}^{N_h} \left[ \frac{v_i - v_j}{2} (\mathbf{f}_j - \mathbf{f}_i) + \mathbf{q}_j + \mathbf{q}_i \right] \cdot \underbrace{\sum_{e \in \mathcal{E}_i} (\mathbf{c}_{ij}^e + \mathbf{c}_{ji}^e)}_{=0} - 2\mathbf{q}_i \cdot \underbrace{\sum_{e \in \mathcal{E}_i} \mathbf{c}_{ii}^e}_{=0} = 0 \end{aligned} \quad (15)$$

in accordance with the fact that  $\frac{d}{dt} \int_{\Omega} \eta(u) \, d\mathbf{x} \leq 0$  for the entropy solution of an initial boundary-value problem with  $\int_{\partial\Omega} \mathbf{q}(u) \cdot \mathbf{n} \, ds = 0$ , where  $\mathbf{n}$  denotes the unit outward normal. Note that the validity of estimate (15) for the square entropy  $\eta = \frac{u^2}{2}$  implies  $L^2$  stability.

Suppose that the exact entropy solution  $u$  belongs to a convex invariant set  $\mathcal{G} = [u^{\min}, u^{\max}]$ . Then a semi-discrete scheme of the form (7) is invariant domain preserving (IDP) if it satisfies

$$u^{\min} \leq u_i^{\min}(t) \leq u_i(t) \leq u_i^{\max}(t) \leq u^{\max} \quad \forall t \geq 0. \quad (16)$$

A fully discrete scheme possesses the IDP property if similar inequality constraints hold at each discrete time level  $t^n = n\Delta t$ ,  $n \in \mathbb{N}$  or stage of a strong stability preserving (SSP) Runge-Kutta method [12]. The following Theorem provides a sufficient condition for the design of IDP approximations.

**Theorem 2** (Guermond-Popov IDP criterion [14, 16]). *Consider a semi-discrete scheme of the form*

$$\sum_{e \in \mathcal{E}_i} m_i^e \frac{du_i}{dt} = \sum_{e \in \mathcal{E}_i} \sum_{j \in \mathcal{N}^e \setminus \{i\}} 2d_{ij}^e (\bar{u}_{ij}^e - u_i), \quad i \in \{1, \dots, N_h\}, \quad (17)$$

where  $m_i^e > 0$  and  $d_{ij}^e > 0$  for all  $j \in \mathcal{N}^e \setminus \{i\}$ . Let  $\mathcal{G}$  be a convex set. Assume that

$$u_i \in \mathcal{G}, \quad \bar{u}_{ij}^e \in \mathcal{G} \quad \forall j \in \mathcal{N}^e \setminus \{i\}. \quad (18)$$

If the time step  $\Delta t$  satisfies

$$\Delta t \sum_{e \in \mathcal{E}_i} \sum_{j \in \mathcal{N}^e \setminus \{i\}} 2d_{ij}^e \leq m_i = \sum_{e \in \mathcal{E}_i} m_i^e, \quad (19)$$

then an explicit SSP Runge-Kutta time discretization of (17) is IDP w.r.t.  $\mathcal{G}$ .

PROOF. Each stage of an explicit SSP-RK method is a forward Euler update of the form

$$\begin{aligned} \bar{u}_i &= u_i + \frac{\Delta t}{m_i} \sum_{e \in \mathcal{E}_i} \sum_{j \in \mathcal{N}^e \setminus \{i\}} 2d_{ij}^e (\bar{u}_{ij}^e - u_i) \\ &= \left( 1 - \frac{\Delta t}{m_i} \sum_{e \in \mathcal{E}_i} \sum_{j \in \mathcal{N}^e \setminus \{i\}} 2d_{ij}^e \right) u_i + \frac{\Delta t}{m_i} \sum_{e \in \mathcal{E}_i} \sum_{j \in \mathcal{N}^e \setminus \{i\}} 2d_{ij}^e \bar{u}_{ij}^e. \end{aligned}$$

Under the time step restriction (19), this representation of the fully discrete scheme implies that  $\bar{u}_i$  is a convex combination of  $u_i \in \mathcal{G}$  and  $\bar{u}_{ij}^e \in \mathcal{G}$ . Since  $\mathcal{G}$  is convex, the result  $\bar{u}_i$  stays in  $\mathcal{G}$  [16].  $\square$

**Remark 1.** After the global residual assembly, the semi-discrete AFC scheme (7) becomes

$$m_i \frac{du_i}{dt} = \sum_{j \in \mathcal{N}_i} [g_{ij} - \mathbf{c}_{ij} \cdot (\mathbf{f}_j - \mathbf{f}_i)], \quad (20)$$

where

$$m_i = \sum_{j \in \mathcal{N}_i} m_{ij}, \quad m_{ij} = \sum_{e \in \mathcal{E}_i \cap \mathcal{E}_j} m_{ij}^e, \quad \mathbf{c}_{ij} = \sum_{e \in \mathcal{E}_i \cap \mathcal{E}_j} \mathbf{c}_{ij}^e. \quad (21)$$

In this paper, we assemble  $g_{ij} = \sum_{e \in \mathcal{E}_i} g_{ij}^e$  from element contributions  $g_{ij}^e$ . However, the corrected flux can also be determined directly. In AFC schemes of this kind, inequality constraints for  $g_{ij}$  are formulated using the coefficients of global matrices (cf. [14, 20, 19, 23]). All algorithms to be presented below can be easily converted to the post-assembly format by dropping the superscript  $e$ .

#### 4. Entropy stable AFC schemes

Let us begin with the derivation of semi-discrete AFC schemes satisfying the entropy stability condition (12). A low-order approximation of local Lax-Friedrichs (LLF) type is defined by

$$g_{ij}^{e,\text{LLF}} = d_{ij}^{e,\text{max}}(u_j - u_i), \quad (22)$$

where

$$d_{ij}^{e,\text{max}} = \begin{cases} \max\{|\mathbf{c}_{ij}^e|, |\mathbf{c}_{ji}^e|\} \max\{\lambda_{ij}^{\text{max}}, \lambda_{ji}^{\text{max}}\} & \text{if } i \in \mathcal{N}^e, j \in \mathcal{N}^e \setminus \{i\}, \\ -\sum_{k \in \mathcal{N}^e \setminus \{i\}} d_{ik}^e & \text{if } j = i \in \mathcal{N}^e, \\ 0 & \text{otherwise} \end{cases} \quad (23)$$

are artificial diffusion coefficients proportional to the maximum wave speed [16, 19, 22]

$$\lambda_{ij}^{\text{max}} = \max_{\omega \in [0,1]} |\mathbf{n}_{ij}^e \cdot \mathbf{f}'(\omega u_i + (1-\omega)u_j)|, \quad \mathbf{n}_{ij}^e = \frac{\mathbf{c}_{ij}^e}{|\mathbf{c}_{ij}^e|}. \quad (24)$$

The LLF flux defined by (22) satisfies (12), as shown by Chen and Shu [8] in the context of entropy stable DG methods. Guermond and Popov [16] proved that the fully discrete SSP-RK version of the LLF-AFC scheme is IDP and satisfies a discrete entropy inequality for any entropy pair  $(\eta, \mathbf{q})$ . However, the accuracy of the LLF approximation is first-order at best and significant amounts of numerical diffusion can be removed without losing the entropy stability property.

To derive a flux control  $g_{ij}^e$  corresponding to a second-order entropy stable approximation, we adopt Tadmor's [32, 33] design philosophy which is based on comparison with entropy conservative schemes. Suppose that condition (12) holds as equality for some  $g_{ij}^{e,\text{EC}}$ . Then it holds as inequality for

$$g_{ij}^{e,\text{ES}} = g_{ij}^{e,\text{EC}} + \nu_{ij}^e(v_j - v_i), \quad (25)$$

where  $\nu_{ij}^e \geq 0$  is an entropy viscosity coefficient. This simple comparison principle provides a powerful tool for the design of entropy stable finite volume [11, 29, 34] and DG [8, 27] methods. For our AFC scheme (7) to be entropy conservative, the fluxes  $g_{ij}^{e,\text{EC}} = -g_{ji}^{e,\text{EC}}$  would need to satisfy

$$\begin{aligned} \frac{v_i - v_j}{2} [g_{ij}^{e,\text{EC}} - \mathbf{c}_{ij}^e \cdot (\mathbf{f}_j + \mathbf{f}_i)] &= \mathbf{c}_{ij}^e \cdot [\boldsymbol{\psi}(u_j) - \boldsymbol{\psi}(u_i)], \\ \frac{v_i - v_j}{2} [g_{ij}^{e,\text{EC}} + \mathbf{c}_{ji}^e \cdot (\mathbf{f}_j + \mathbf{f}_i)] &= \mathbf{c}_{ji}^e \cdot [\boldsymbol{\psi}(u_i) - \boldsymbol{\psi}(u_j)]. \end{aligned}$$

Since this system is overdetermined in the case  $\mathbf{c}_{ij}^e \neq -\mathbf{c}_{ji}^e$ , we perform element-level flux correction using generalized entropy-stable target fluxes of the form

$$g_{ij}^{e,\text{ES}} = d_{ij}^{e,\text{min}}(u_j - u_i) + \nu_{ij}^e(v_j - v_i), \quad (26)$$

where  $d_{ij}^{e,\text{min}} \in [0, d_{ij}^{e,\text{max}}]$  is the minimal nonnegative diffusion coefficient satisfying the symmetry condition  $d_{ij}^{e,\text{min}} = d_{ji}^{e,\text{min}}$  and condition (12) for both nodes. The value of  $d_{ij}^{e,\text{min}}$  is given by

$$d_{ij}^{e,\text{min}} = \begin{cases} \frac{\min\{Q_{ij}^e, 0, Q_{ji}^e\}}{(v_i - v_j)(u_j - u_i)} & \text{if } u_i \neq u_j, \\ 0 & \text{if } u_i = u_j, \end{cases} \quad (27)$$

where

$$Q_{ij}^e = 2\mathbf{c}_{ij}^e \cdot \left[ \boldsymbol{\psi}(u_j) - \boldsymbol{\psi}(u_i) + (v_i - v_j) \frac{\mathbf{f}_j + \mathbf{f}_i}{2} \right]. \quad (28)$$

By the mean value theorem, we have  $v_i - v_j = \eta'(u_i) - \eta'(u_j) = \eta''(\xi)(u_i - u_j)$  for some  $\xi \in \mathbb{R}$ . It follows that  $(v_i - v_j)(u_j - u_i) \leq 0$  and, therefore,  $d_{ij}^{e,\text{min}} \geq 0$  for any convex entropy  $\eta$ .

**Remark 2.** In the absence of rounding errors, we have  $d_{ij}^{e,\text{min}} \leq d_{ij}^{e,\text{max}}$  by definition. In practice, division by a small number  $(v_i - v_j)(u_j - u_i)$  may produce  $d_{ij}^{e,\text{min}} > d_{ij}^{e,\text{max}}$  in regions where the numerical solution is almost constant. To avoid this, it is worthwhile to use  $d_{ij}^{e,\text{max}}$  as upper bound for  $d_{ij}^{e,\text{min}}$  in practical implementations. We also remark that the direct calculation of the diffusive flux  $d_{ij}^{e,\text{min}}(u_j - u_i) = \frac{\min\{Q_{ij}^e, 0, Q_{ji}^e\}}{v_i - v_j}$  is less sensitive to rounding errors in the limit  $|u_i - u_j| \rightarrow 0$ .

The AFC scheme corresponding to (26) with  $\nu_{ij}^e = 0$  is *barely entropy stable*. Building on Tadmor's [33] ideas, we define the additional flux  $\nu_{ij}^e(v_j - v_i)$  using the entropy viscosity coefficient

$$\nu_{ij}^e = \max \left\{ \frac{\mathbf{c}_{ij}^e \cdot \left[ \mathbf{f}_j + \mathbf{f}_i - 2\mathbf{f} \left( \frac{u_j + u_i}{2} \right) \right]}{v_j - v_i}, 0, \frac{\mathbf{c}_{ji}^e \cdot \left[ \mathbf{f}_j + \mathbf{f}_i - 2\mathbf{f} \left( \frac{u_j + u_i}{2} \right) \right]}{v_i - v_j} \right\} \quad (29)$$

which vanishes for linear flux functions  $\mathbf{f}(u)$  and preserves second-order accuracy for nonlinear ones.

**Remark 3.** For reasons explained in Remark 2, we recommend direct calculation of the flux

$$\nu_{ij}^e(v_j - v_i) = S_{ij} \max \{ S_{ij} \mathbf{c}_{ij}^e \cdot 2\Delta\mathbf{f}_{ij}, 0, -S_{ij} \mathbf{c}_{ji}^e \cdot 2\Delta\mathbf{f}_{ij} \}, \quad (30)$$

where  $S_{ij}$  is the sign of  $v_j - v_i$  and  $\Delta\mathbf{f}_{ij} = \frac{1}{2}(\mathbf{f}_j + \mathbf{f}_i) - \mathbf{f} \left( \frac{u_j + u_i}{2} \right)$  is the flux difference.

The use of (26) with  $d_{ij}^{e,\text{min}}$  defined by (27) and  $\nu_{ij}^e$  defined by (29) yields an entropy stable approximation which exhibits the desired convergence behavior for smooth data but may produce undershoots and/or overshoots in the neighborhood of shocks. To enforce the IDP property and preservation of local bounds, we use the monolithic convex limiting techniques presented in the next section.

## 5. Bound-preserving AFC schemes

The highly dissipative LLF flux (22) satisfies not only the entropy condition (12) but also the assumptions of Theorem 2. The corresponding IDP bar states are given by

$$\bar{u}_{ij}^e = \frac{u_j + u_i}{2} - \frac{\mathbf{c}_{ij}^e \cdot (\mathbf{f}_j - \mathbf{f}_i)}{2d_{ij}^{e,\max}}, \quad (31)$$

where  $d_{ij}^{e,\max}$  is defined by (23). Using the mean value theorem, one can show that [19]

$$\min\{u_i, u_j\} \leq \bar{u}_{ij}^e \leq \max\{u_i, u_j\}. \quad (32)$$

Hence, the algebraic LLF scheme is IDP by Theorem 2. To limit the raw antidiffusive part

$$f_{ij}^e = g_{ij}^e - g_{ij}^{e,\text{LLF}} \quad (33)$$

of a given flux control  $g_{ij}^e$  in a manner which preserves the IDP property, we define

$$g_{ij}^{e,*} = g_{ij}^{e,\text{LLF}} + f_{ij}^{e,*} = d_{ij}^{e,\max}(u_j - u_i) + f_{ij}^{e,*} \quad (34)$$

using the inequality-constrained antidiffusive flux [19, 22]

$$f_{ij}^{e,*} = \begin{cases} \min \left\{ f_{ij}^e, 2d_{ij}^e \min \{ u_i^{\max} - \bar{u}_{ij}^e, \bar{u}_{ji}^e - u_j^{\min} \} \right\} & \text{if } f_{ij}^e > 0, \\ \max \left\{ f_{ij}^e, 2d_{ij}^e \max \{ u_i^{\min} - \bar{u}_{ij}^e, \bar{u}_{ji}^e - u_j^{\max} \} \right\} & \text{otherwise.} \end{cases} \quad (35)$$

This monolithic convex limiting (MCL) strategy was proposed in [19]. It guarantees that

$$\min_{j \in \mathcal{N}_i} u_j =: u_i^{\min} \leq \bar{u}_{ij}^{e,*} = \bar{u}_{ij}^e + \frac{f_{ij}^{e,*}}{2d_{ij}^{e,\max}} \leq u_i^{\max} := \max_{j \in \mathcal{N}_i} u_j. \quad (36)$$

The IDP property of the flux-corrected scheme can be shown using Theorem 2, see [19] for details.

**Remark 4.** A linearity-preserving version of the bounds  $u_i^{\min}$  and  $u_i^{\max}$  can be constructed as proposed in Section 6.1 of [19]. The use of limiters that guarantee linearity preservation (i.e., produce  $f_{ij}^{e,*} = f_{ij}^e$  for locally linear functions  $u_h$ ) is essential for achieving optimal convergence to smooth solutions [4].

Formula (35) will leave the raw antidiffusive flux  $f_{ij}^e$  unchanged if it does not violate the AFC inequality constraints (36). Hence, the quality of flux-corrected solutions depends on the properties of the (stabilized) high-order method defined by (7) with  $g_{ij}^e = g_{ij}^{e,\text{LLF}} + f_{ij}^e$ . The target flux

$$f_{ij}^e = (d_{ij}^{e,\min} - d_{ij}^{e,\max})(u_j - u_i) + \nu_{ij}^e(v_j - v_i) \quad (37)$$

corresponds to an entropy stable lumped-mass approximation. The addition of (37) to  $g_{ij}^{e,\text{LLF}}$  replaces it with  $g_{ij}^{e,\text{ES}}$ . If limiting is performed using (35), the addition of  $f_{ij}^{e,*}$  replaces  $g_{ij}^{e,\text{LLF}}$  with

$$g_{ij}^{e,*} = (1 - \alpha_{ij}^e) d_{ij}^{e,\text{max}}(u_j - u_i) + \alpha_{ij}^e g_{ij}^{e,\text{ES}}, \quad \alpha_{ij}^e = \begin{cases} \frac{f_{ij}^{e,*}}{f_{ij}^e} & \text{if } f_{ij}^e \neq 0, \\ 0 & \text{otherwise.} \end{cases} \quad (38)$$

Recall that  $(v_i - v_j)(u_j - u_i) \leq 0$  for any convex entropy  $\eta$  by the mean value theorem and definition of the entropy variable  $v = \eta'(u)$ . Since  $\alpha_{ij}^e \in [0, 1]$  and  $d_{ij}^{e,\text{max}} \geq d_{ij}^{e,\text{min}}$ , we have

$$\begin{aligned} (v_i - v_j) g_{ij}^{e,*} &= (v_i - v_j) [(1 - \alpha_{ij}^e) d_{ij}^{e,\text{max}}(u_j - u_i) + \alpha_{ij}^e d_{ij}^{e,\text{min}}(u_j - u_i) + \alpha_{ij}^e \nu_{ij}^e (v_j - v_i)] \\ &\leq (v_i - v_j) d_{ij}^{e,\text{min}}(u_j - u_i). \end{aligned}$$

Thus the replacement of  $g_{ij}^{e,\text{LLF}}$  by  $g_{ij}^{e,*}$  produces an entropy stable and bound-preserving approximation.

In the consistent-mass version of our AFC scheme, the target flux to be used in (35) is given by

$$f_{ij}^e = m_{ij}^e (\dot{u}_i - \dot{u}_j) + (d_{ij}^{e,\text{min}} - d_{ij}^{e,\text{max}})(u_j - u_i) + \nu_{ij}^e (v_j - v_i) \quad (39)$$

and represents the antidiffusive part of  $g_{ij}^e = g_{ij}^{e,\text{CG}} + g_{ij}^{e,\text{ES}}$ . The nodal time derivatives  $\dot{u}$  can be defined using (5) or (7). In the numerical examples of Section 7, we use the LLF approximation

$$\dot{u}_i = \frac{1}{m_i} \sum_{e \in \mathcal{E}_i} \sum_{j \in \mathcal{N}^e \setminus \{i\}} [d_{ij}^{e,\text{max}}(u_j - u_i) - \mathbf{c}_{ij}^e \cdot (\mathbf{f}_j - \mathbf{f}_i)]. \quad (40)$$

In addition to being rather inexpensive, it has the positive effect of introducing high-order background stabilization [19] even for linear advection problems, for which  $\nu_{ij}^e$  defined by (29) vanishes.

The inclusion of  $m_{ij}^e (\dot{u}_i - \dot{u}_j)$  may require additional limiting of  $f_{ij}^{e,*}$  to ensure that the final flux

$$g_{ij}^{e,**} = g_{ij}^{e,\text{LLF}} + f_{ij}^{e,**} = d_{ij}^{e,\text{max}}(u_j - u_i) + f_{ij}^{e,**} \quad (41)$$

of our property-preserving AFC scheme (7) will satisfy the entropy stability condition

$$\frac{v_i - v_j}{2} [g_{ij}^{e,**} - \mathbf{c}_{ij}^e \cdot (\mathbf{f}_j + \mathbf{f}_i)] \leq \mathbf{c}_{ij}^e \cdot [\boldsymbol{\psi}(u_j) - \boldsymbol{\psi}(u_i)]. \quad (42)$$

Substituting (41) into (42), we obtain a limiting criterion for the algebraic entropy flux

$$f_{ij}^{e,**} = \begin{cases} \frac{\min\{Q_{ij}^{e,*}, (v_i - v_j) f_{ij}^{e,*}, Q_{ji}^{e,*}\}}{v_i - v_j} & \text{if } (v_i - v_j) f_{ij}^{e,*} > 0, \\ f_{ij}^{e,*} & \text{otherwise,} \end{cases} \quad (43)$$

where

$$Q_{ij}^{e,*} = Q_{ij}^e - (v_j - v_i) d_{ij}^{e,\text{max}}(u_i - u_j) \quad (44)$$

are upper bounds for entropy-producing fluxes. The value of  $Q_{ij}^e$  is given by (28). Note that

$$Q_{ij}^{e,*} \geq (v_i - v_j) (d_{ij}^{e,\text{max}} - d_{ij}^{e,\text{min}})(u_i - u_j) = \eta''(\xi) (d_{ij}^{e,\text{max}} - d_{ij}^{e,\text{min}})(u_i - u_j)^2$$

for some  $\xi \in \mathbb{R}$ . Since  $d_{ij}^{e,\text{max}} \geq d_{ij}^{e,\text{min}}$ , the bounds  $Q_{ij}^{e,*}$  are nonnegative for any convex entropy  $\eta$ .

**Remark 5.** The replacement of  $f_{ij}^{e,*}$  by the entropy-corrected flux  $f_{ij}^{e,**}$  is equivalent to multiplication by a correction factor  $\alpha_{ij}^e \in [0, 1]$ . Hence, it does not affect the IDP property of our AFC scheme.

## 6. Summary of the algorithm

Let us now summarize the algorithmic steps to be performed and the properties of the AFC scheme that ensures entropy stability and preservation of local bounds. At the semi-discrete level, the flux-corrected CG approximation is defined by the nonlinear system of ordinary differential equations

$$m_i \frac{du_i}{dt} = \sum_{e \in \mathcal{E}_i} \sum_{j \in \mathcal{N}^e \setminus \{i\}} [d_{ij}^{e,\max}(u_j - u_i) + f_{ij}^{e,**} - \mathbf{c}_{ij}^e \cdot (\mathbf{f}_j - \mathbf{f}_i)], \quad i = 1, \dots, N_h, \quad (45)$$

where  $d_{ij}^{e,\max}$  is the maximal speed diffusion coefficient defined by (23). If all corrections are included, the computation of the limited antidiffusive flux  $f_{ij}^{e,**}$  involves the following steps:

1. Calculate the minimal diffusion coefficient  $d_{ij}^{e,\min}$  using (27).
2. Calculate the entropy viscosity coefficient  $\nu_{ij}^e$  using (29).
3. Calculate the approximate time derivatives  $\dot{u}_i$  using (40).
4. Calculate the raw antidiffusive fluxes  $f_{ij}^e$  using (39).
5. Calculate the local bounds  $u_i^{\max}$  and  $u_i^{\min}$  using (36).
6. Calculate the bound-preserving fluxes  $f_{ij}^{e,*}$  using (35).
7. Calculate the entropy-corrected fluxes  $f_{ij}^{e,**}$  using (43).

The following implication of Theorem 2 provides a sufficient condition for an explicit time discretization of the nonlinear semi-discrete AFC problem (45) to be locally bound preserving.

**Theorem 3** (IDP property of the flux-corrected CG scheme). *An explicit SSP Runge-Kutta time discretization of system (45) satisfies the local maximum principle*

$$u_i^{\min} \leq \bar{u}_i \leq u_i^{\max} \quad (46)$$

under the time step restriction

$$\Delta t \sum_{e \in \mathcal{E}_i} \sum_{j \in \mathcal{N}^e \setminus \{i\}} 2d_{ij}^{e,\max} \leq m_i. \quad (47)$$

PROOF. To apply Theorem 2, we notice that each SSP Runge-Kutta stage can be written as (cf. [19])

$$\bar{u}_i = u_i + \frac{\Delta t}{m_i} \sum_{e \in \mathcal{E}_i} \sum_{j \in \mathcal{N}^e \setminus \{i\}} 2d_{ij}^{e,\max} (\bar{u}_{ij}^{e,**} - u_i), \quad (48)$$

where

$$u_i^{\min} \leq \bar{u}_{ij}^{e,**} = \bar{u}_{ij}^e + \frac{f_{ij}^{e,**}}{2d_{ij}^{e,\max}} \leq u_i^{\max} \quad (49)$$

by virtue of (32), (35), and (43). The desired result follows by the convexity argument.  $\square$

**Remark 6.** The applicability of the presented AFC tools is not restricted to explicit SSP Runge-Kutta time discretizations. Nonlinear discrete problems associated with implicit time discretizations and the steady state limit of (45) can be analyzed as in [5, 24], see also the Appendix of [19].

## 7. Numerical examples

In this section, we perform numerical experiments for linear and nonlinear scalar problems. The purpose of this numerical study is to demonstrate that the proposed methodology provides optimal accuracy for linear ( $\mathbb{P}_1$ ) and multilinear ( $\mathbb{Q}_1$ ) finite element approximations to smooth solutions, and that it behaves as expected on structured as well as unstructured meshes. In the description of the numerical results, we use the abbreviation LO-ES-IDP for the low-order LLF scheme defined by (7) and (22). The high-order entropy stable IDP scheme of Section 6 is labeled HO-ES-IDP. The method corresponding to HO-ES-IDP without Step 6 is referred to as HO-ES. We use this version to show the effect of deactivating the IDP limiter. The significance of individual steps of the HO-ES-IDP algorithm is further illustrated by varying the definition of the target flux  $f_{ij}^e$  for a two-dimensional test problem with a nonconvex flux function (the so-called KPP problem [18]). In all numerical examples, we discretize in time using the third-order explicit SSP Runge-Kutta method with three stages [12]. Unless otherwise stated, we use structured triangular meshes. All computations are performed using Proteus (<https://proteustoolkit.org>), an open-source Python toolkit for numerical simulations.

### 7.1. One-dimensional advection

The first problem that we consider in this work is the one-dimensional linear advection equation

$$\frac{\partial u}{\partial t} + a \frac{\partial u}{\partial x} = 0 \quad \text{in } \Omega = (0, 1) \quad (50)$$

with the constant velocity  $a = 1$ . The smooth initial condition is given by

$$u_0(x) = \cos(2\pi(x - 0.5)). \quad (51)$$

We solve (50) up to the final time  $t = 1$  and measure the numerical errors w.r.t. the  $L^1$  norm. In Table 1, we show the results of a grid convergence study. As expected, LO-ES-IDP exhibits first-order convergence behavior, while second-order convergence is achieved with HO-ES and HO-ES-IDP.

### 7.2. Two-dimensional advection

The next example was used in [3] to study the numerical behavior of flux-corrected transport algorithms for high-order DG discretizations of the two-dimensional linear advection problem

$$\frac{\partial u}{\partial t} + \mathbf{v} \cdot \nabla u = 0 \quad \text{in } \Omega = (0, 100)^2 \quad (52)$$

with constant velocity  $\mathbf{v} = (10, 10)$ . The initial condition, which is shown in Figure 1b, is composed of two rings and a cross. The upper ring is centered at  $(x, y) = (40, 40)$ . The radii of its inner and outer

$N_h$	LO-ES-IDP		HO-ES		HO-ES-IDP	
	$\ u_h - u_{\text{exact}}\ _{L^1}$	EOC	$\ u_h - u_{\text{exact}}\ _{L^1}$	EOC	$\ u_h - u_{\text{exact}}\ _{L^1}$	EOC
11	3.70E-2	–	1.21E-2	–	1.69E-2	–
16	2.92E-2	0.58	6.01E-3	1.73	8.32E-3	1.74
21	2.40E-2	0.68	3.73E-3	1.65	5.15E-3	1.66
31	1.77E-2	0.75	1.82E-3	1.76	2.51E-3	1.77
41	1.40E-2	0.81	1.08E-3	1.81	1.47E-3	1.84
61	9.84E-3	0.86	5.06E-4	1.86	6.93E-4	1.86
81	7.59E-3	0.90	2.95E-4	1.88	4.01E-4	1.90
121	5.21E-3	0.92	1.36E-4	1.89	1.87E-4	1.88
161	3.97E-3	0.94	7.86E-5	1.91	1.08E-4	1.90
241	2.68E-3	0.96	3.65E-5	1.89	4.94E-5	1.92
321	2.03E-3	0.97	2.11E-5	1.90	2.82E-5	1.94
481	1.36E-3	0.98	9.69E-6	1.91	1.28E-5	1.95

Table 1: One-dimensional advection. Grid convergence history for three entropy-stable AFC schemes.

circles are 7 and 10, respectively. The center of the lower ring is located at the point  $(x, y) = (40, 20)$ . The radii of the inner and outer circles are 3 and 7, respectively. The cross occupies the region  $r_1 \cup r_2 \subset \Omega$ , where  $r_1 = \{x, y \in \Omega \mid x \in [7, 32], y \in [10, 13]\}$  and  $r_2 = \{x, y \in \Omega \mid x \in [14, 17], y \in [3, 26]\}$ , rotated by  $-45^\circ$  around the point  $(x, y) = (15.5, 11.5)$ .

For this problem, we use unstructured grids. In Figure 1a, we show a zoom of one of these grids. Computations are terminated at the final time  $t = 4$ . In Figures 1c and 1d, we present the LO-ES-IDP and HO-ES solutions calculated using  $N_h = 99,412$  degrees of freedom (DoFs). The higher accuracy of the latter approximation illustrates the need for antidiffusive corrections of the LLF flux. No significant undershoots or overshoots are generated by HO-ES in this example. The results obtained with the HO-ES-IDP scheme on three successively refined meshes are shown in Figure 2. The advected discontinuities are resolved in a crisp and nonoscillatory manner, especially on the finest mesh.

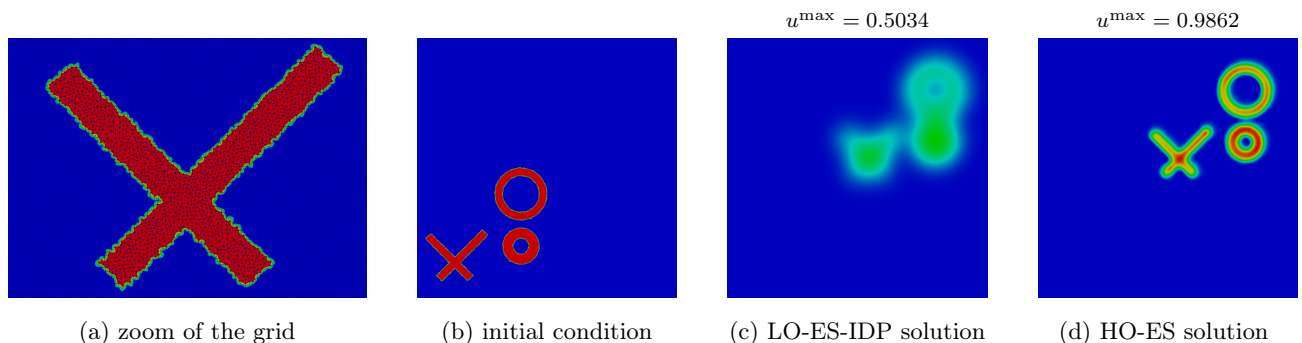


Figure 1: Two-dimensional linear advection problem. Zoom of the unstructured grid, initial data, and numerical solutions at  $t = 4$  obtained with  $N_h = 99,412$  DoFs.

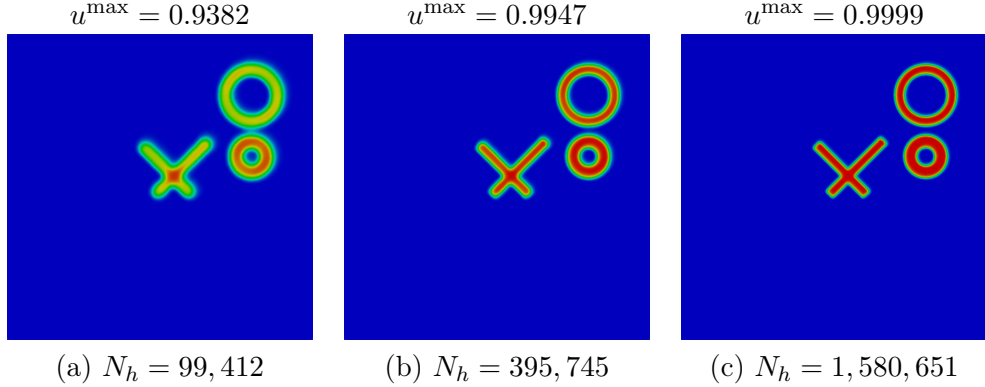


Figure 2: Two-dimensional linear advection problem. Numerical solutions at  $t = 4$  obtained with HO-ES-IDP on three successively refined unstructured grids.

### 7.3. KPP problem

The KPP problem [16, 17, 18] is a challenging nonlinear test for verification of entropy stability properties. We use this problem to test different components of the method that we propose. In this series of 2D experiments, we solve equation (1a) with the nonlinear and nonconvex flux function

$$\mathbf{f}(u) = (\sin(u), \cos(u)) \quad (53)$$

in the computational domain  $\Omega = (-2, 2) \times (-2.5, 1.5)$  using the initial condition

$$u_0(x, y) = \begin{cases} \frac{14\pi}{4} & \text{if } \sqrt{x^2 + y^2} \leq 1, \\ \frac{\pi}{4} & \text{otherwise.} \end{cases} \quad (54)$$

A simple (but rather pessimistic) upper bound for the guaranteed maximum speed (GMS) is  $\lambda = 1$ . More accurate GMS estimates can be found in [17]. The exact solution exhibits a two-dimensional rotating wave structure, which is difficult to capture in numerical simulations using high-order methods. The main challenge of this test is to prevent possible convergence to wrong weak solutions.

Numerical solutions are evolved up to the final time  $t = 1$ . To test individual components of the AFC scheme summarized in Section 6, we vary the definition of the target flux  $f_{ij}^e$  and/or the way in which it is limited to produce a constrained flux  $f_{ij}^{e,**}$ . In Figure 3a, we present the LO-ES-IDP solution ( $f_{ij}^{e,**} = 0 = f_{ij}^e$ ). It is highly dissipative but provides a correct qualitative description of the rotating wave structure. The solution displayed in Figure 3b was calculated using  $f_{ij}^{e,**} = d_{ij}^e(u_i - u_j) = f_{ij}^e$ . This lumped-mass Galerkin approximation is highly oscillatory and exhibits an entropy-violating merger of two shocks. The solutions shown in Figures 3c and 3d were obtained using the IDP-limited counterparts  $f_{ij}^{e,**} = f_{ij}^{e,*}$  of  $f_{ij}^e = d_{ij}^e(u_i - u_j)$  and  $f_{ij}^e = m_{ij}^e(\dot{u}_i - \dot{u}_j) + d_{ij}^e(u_i - u_j)$ , respectively. As reported in [19, 24], the latter definition of the target flux introduces high-order background dissipation. However, neither the activation of the IDP limiter nor the inclusion of  $m_{ij}^e(\dot{u}_i - \dot{u}_j)$  provides enough entropy dissipation to capture the twisted shocks correctly in the KPP test. This unsatisfactory state of affairs

illustrates the need for entropy stabilization and confirms the findings of Guermond et al. [16] who noticed that IDP limiting alone does not guarantee convergence to entropy solutions.

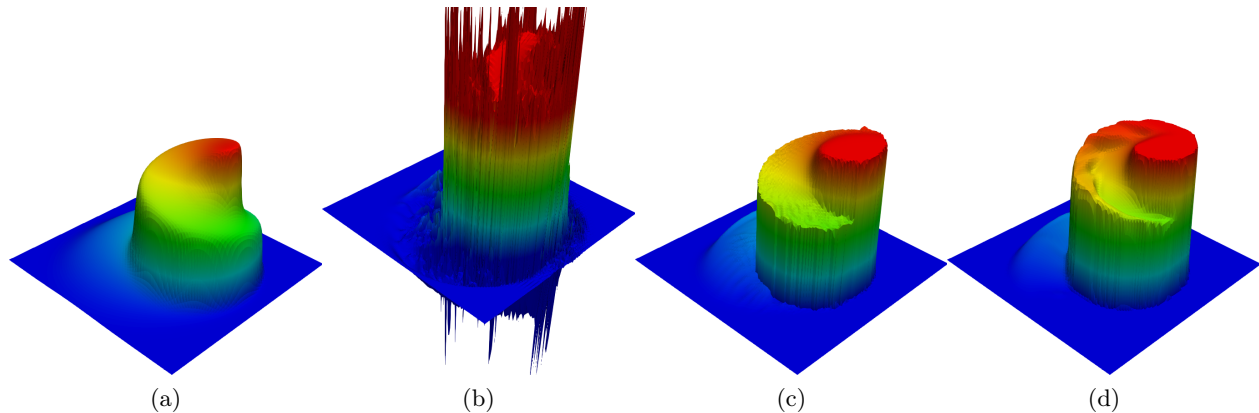


Figure 3: Numerical solutions of the KPP problem at  $t = 1$  obtained using  $N_h = 129^2$  DoFs and (a) LO-ES-IDP, (b) unconstrained lumped-mass Galerkin method corresponding to  $f_{ij}^{e,**} = d_{ij}^{e,max}(u_i - u_j) = f_{ij}^e$ , (c) IDP limiter (35) for  $f_{ij}^e = d_{ij}^{e,max}(u_i - u_j)$ , and (d) IDP limiter (35) for  $f_{ij}^e = m_{ij}^e(\dot{u}_i - \dot{u}_j) + d_{ij}^{e,max}(u_i - u_j)$ .

In Figure 4, we present numerical solutions produced by three entropy stable high-order methods using  $N_h = 129^2$ . Each column corresponds to a different definition of the target flux  $f_{ij}^e$ . The diagrams of the first row were calculated without invoking the IDP flux limiter (35). Therefore, the results exhibit undershoots/overshoots. The target fluxes of the three schemes under investigation are listed in the caption. The use of  $f_{ij}^e = (d_{ij}^{e,min} - d_{ij}^{e,max})(u_j - u_i)$  produces a barely entropy stable approximation which requires additional entropy fixes to keep the shocks separated if no IDP constraints are imposed. The inclusion of  $\nu_{ij}^e(v_j^n - v_i^n)$  and  $m_{ij}^e(\dot{u}_i - \dot{u}_j)$  leads to AFC schemes that reproduce the rotating wave structure correctly even without IDP limiting. The method employed in the last diagram of the second row is HO-ES-IDP. In Figure 5, we show the HO-ES-IDP results for finer meshes. As the number of degrees of freedom is increased, the method converges to a bound-preserving entropy solution.

#### 7.4. Inviscid Burgers equation

Let us now consider the two-dimensional inviscid Burgers equation [13, 19]

$$\frac{\partial u}{\partial t} + \nabla \cdot \left( \mathbf{v} \frac{u^2}{2} \right) = 0 \quad \text{in } \Omega = (0, 1)^2, \quad (55)$$

where  $\mathbf{v} = (1, 1)$  is a constant vector. The piecewise-constant initial data is given by

$$u_0(x, y) = \begin{cases} -0.2 & \text{if } x < 0.5 \wedge y > 0.5, \\ -1.0 & \text{if } x > 0.5 \wedge y > 0.5, \\ 0.5 & \text{if } x < 0.5 \wedge y < 0.5, \\ 0.8 & \text{if } x > 0.5 \wedge y < 0.5. \end{cases} \quad (56)$$

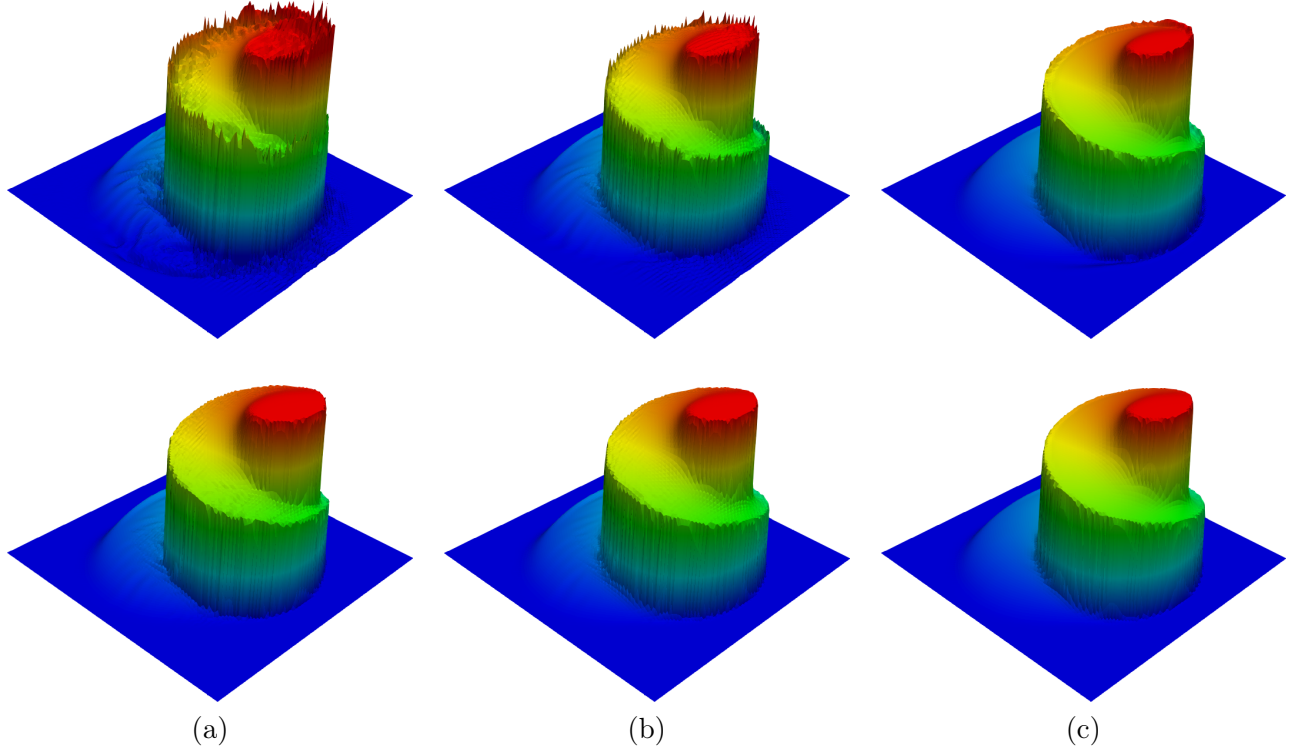


Figure 4: Numerical solutions of the KPP problem obtained at  $t = 1$  using  $N_h = 129^2$  DoFs. The diagrams of the first and second rows show the results produced by three entropy stable high-order schemes without and with activation of the IDP flux limiter, respectively. The target fluxes are defined by (a)  $f_{ij}^e = (d_{ij}^{e,\min} - d_{ij}^{e,\max})(u_j^n - u_i^n)$  for the diagrams of the first column, (b)  $f_{ij}^e = (d_{ij}^{e,\min} - d_{ij}^{e,\max})(u_j^n - u_i^n) + \nu_{ij}^e(v_j^n - v_i^n)$  for the diagrams of the second column, and (c)  $f_{ij}^e = m_{ij}^e(\dot{u}_i - \dot{u}_j) + (d_{ij}^{e,\min} + d_{ij}^{e,\max})(u_j - u_i) + \nu_{ij}^e(v_j - v_i)$  for the diagrams of the third column.

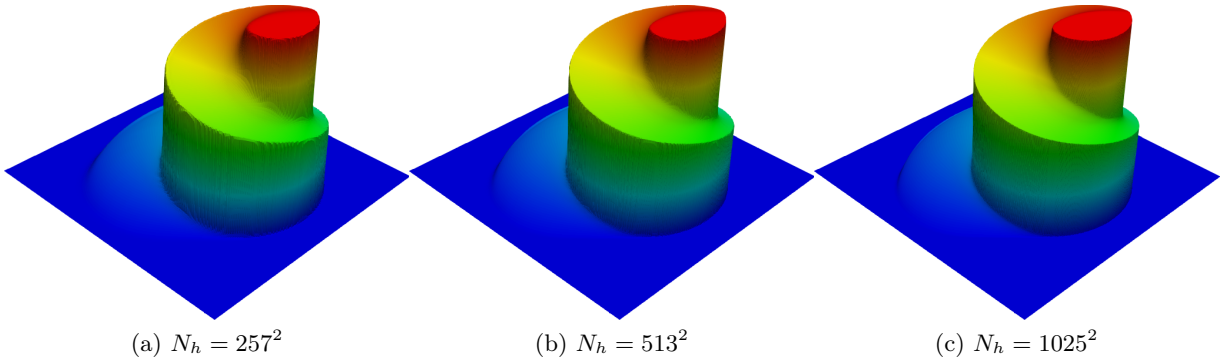


Figure 5: Numerical solutions of the KPP problem at  $t = 1$  obtained using HO-ES-IDP on three meshes.

The inflow boundary conditions are defined using the exact solution of the pure initial value problem in  $\mathbb{R}^2$ . This solution can be found in [13] and stays in the invariant set  $\mathcal{G} = [-1.0, 0.8]$ .

The final time for computation of numerical solutions is  $t = 0.5$ . In Table 2, we show the results of a grid convergence study for LO-ES-IDP, HO-ES, and HO-ES-IDP. In this example, the low-order LLF scheme performs remarkably well at self-steepening shocks but the resolution of rarefactions is not as accurate as in the case of the high-order entropy stable method without and with IDP limiting. The HO-ES-IDP results calculated on three successively refined meshes are displayed in Figure 6.

	LO-ES-IDP		HO-ES		HO-ES-IDP	
$N_h$	$\ u_h - u_{\text{exact}}\ _{L^1}$	EOC	$\ u_h - u_{\text{exact}}\ _{L^1}$	EOC	$\ u_h - u_{\text{exact}}\ _{L^1}$	EOC
$33^2$	7.63E-2	–	4.02E-2	–	3.93E-2	–
$65^2$	4.49E-2	0.76	2.12E-2	0.92	2.09E-2	0.91
$129^2$	2.51E-2	0.85	1.11E-2	0.95	1.10E-2	0.95
$257^2$	1.37E-2	0.85	5.57E-3	0.97	5.62E-3	0.94
$513^2$	7.31E-3	0.90	2.80E-3	0.99	2.83E-3	0.98

Table 2: Inviscid Burgers equation in two dimensions. Grid convergence history for three entropy stable AFC schemes.

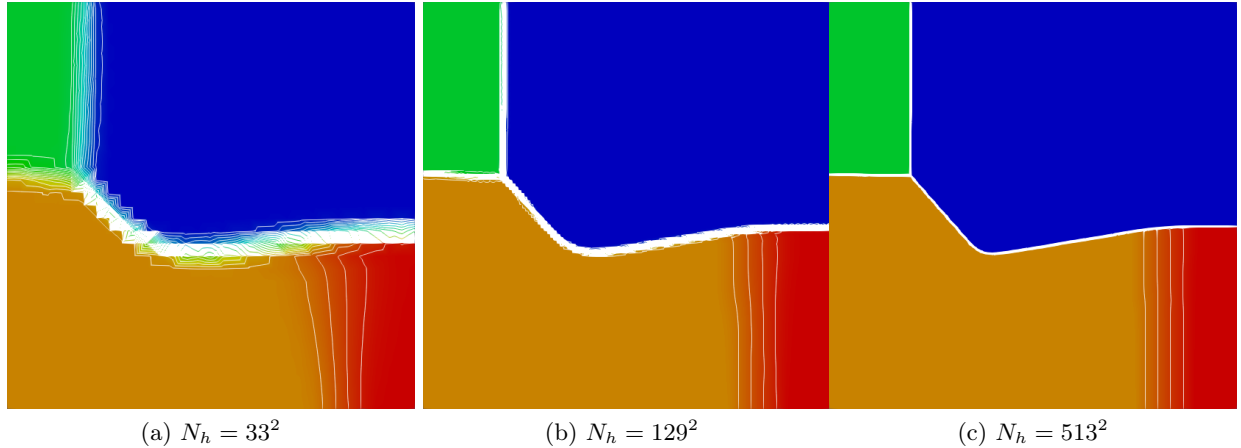


Figure 6: Inviscid Burgers equation in two dimensions. Numerical solutions at  $t = 0.5$  obtained with HO-ES-IDP on three meshes. In each diagram, we plot 30 contour lines corresponding to a uniform subdivision of  $\mathcal{G} = [-1.0, 0.8]$ .

### 7.5. Buckley-Leverett equation

In the last numerical experiment, we consider the two-dimensional Buckley-Leverett equation. The nonconvex flux function of the nonlinear conservation law to be solved is [9]

$$\mathbf{f}(u) = \frac{u^2}{u^2 + (1-u)^2} \begin{bmatrix} 1 \\ 1 - 5(1-u)^2 \end{bmatrix}. \quad (57)$$

The computational domain is  $\Omega = (-1.5, 1.5)^2$ . The initial condition is given by

$$u_0(x, y) = \begin{cases} 1 & \text{if } x^2 + y^2 < 0.5, \\ 0 & \text{otherwise.} \end{cases} \quad (58)$$

An upper bound for the fastest wave speed can be found in [9]. Similarly to the KPP problem, the solution exhibits a rotating wave structure. In Figure 7, we show the entropy stable AFC approximations at the final time  $t = 0.5$ . Note that small oscillations are present if the IDP flux limiter is not applied. The effect of mesh refinement on the accuracy of HO-ES-IDP is illustrated by the snapshots presented in Figure 8. In all experiments for this test problem we use bilinear finite elements.

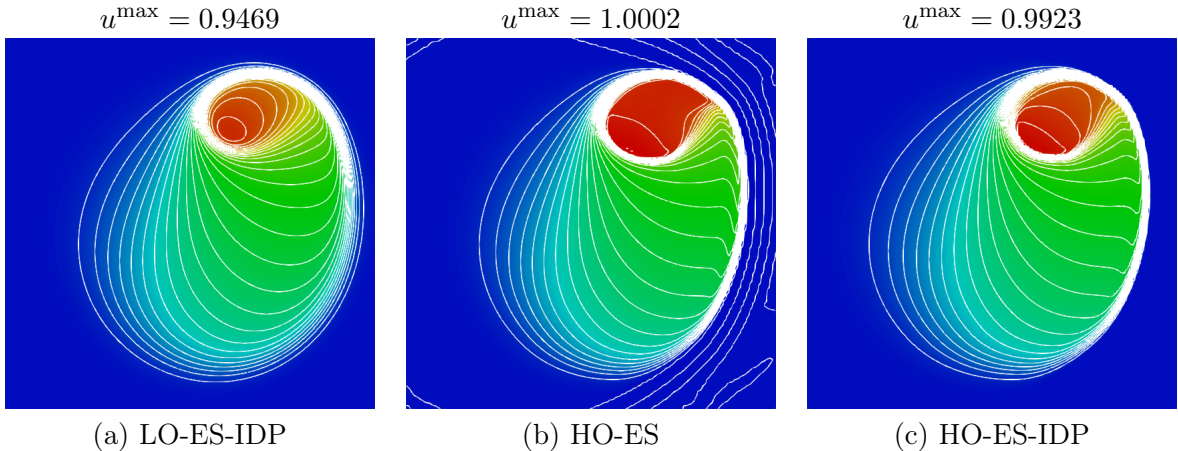


Figure 7: Two-dimensional Buckley-Leverett problem. Numerical solutions at  $t = 0.5$  obtained with three entropy-stable AFC schemes using  $\mathbb{Q}_1$  finite elements and  $N_h = 129^2$  DoFs. In each diagram, we plot 30 contour lines corresponding to a uniform subdivision of  $\mathcal{G} = [0, 1]$ .

## 8. Conclusions

We have shown that algebraic flux correction schemes can be configured to satisfy discrete entropy inequalities in addition to discrete maximum principles. The new inequality-constrained stabilization techniques modify the residual of the semi-discrete Galerkin scheme in a way which ensures entropy stability while preserving all other important properties (conservation, preservation of local bounds, low levels of numerical diffusion). The proposed methodology was presented in the context of continuous Galerkin methods. Further developments will focus on the DG version [1, 2, 8, 27], extensions to high-order finite elements [3, 22], and design of entropy stability preserving time integrators [28].

**Acknowledgments.** The work of Dmitri Kuzmin was supported by the German Research Association (DFG) under grant KU 1530/23-1. The authors would like to thank Hennes Hajduk (TU Dortmund University) for careful proofreading of the manuscript and helpful feedback.

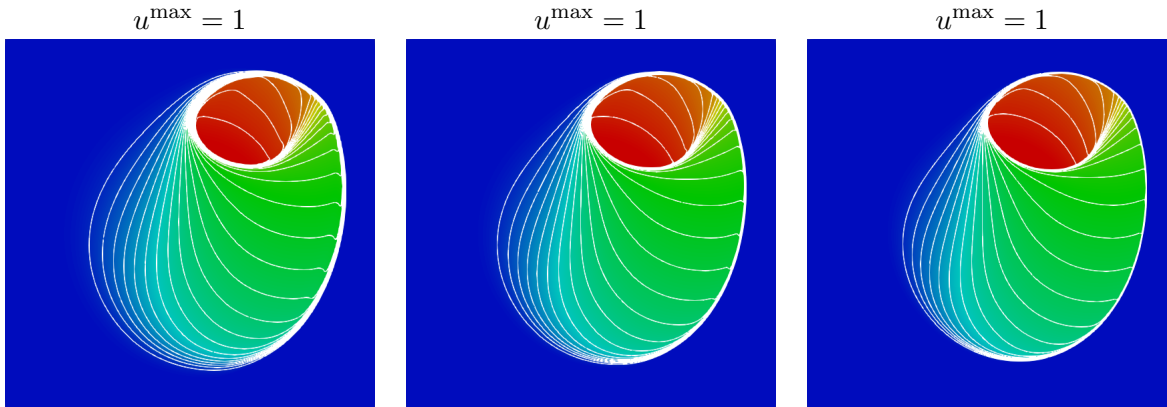


Figure 8: Two-dimensional Buckley-Leverett problem. Numerical solutions at  $t = 0.5$  obtained with HO-ES-IDP on three meshes. In each diagram, we plot 30 contour lines corresponding to a uniform subdivision of  $\mathcal{G} = [0, 1]$ .

## References

- [1] R. Abgrall, A general framework to construct schemes satisfying additional conservation relations. Application to entropy conservative and entropy dissipative schemes. *J. Comput. Phys.* **372** (2018) 640–666.
- [2] R. Abgrall, P. Öffner, and H. Ranocha, Reinterpretation and extension of entropy correction terms for residual distribution and discontinuous Galerkin schemes. Preprint [arXiv: 1908.04556v1](https://arxiv.org/abs/1908.04556v1), 2019
- [3] R. Anderson, V. Dobrev, Tz. Kolev, D. Kuzmin, M. Quezada de Luna, R. Rieben, and V. Tomov, High-order local maximum principle preserving (MPP) discontinuous Galerkin finite element method for the transport equation. *J. Comput. Phys.* **334** (2017) 102–124.
- [4] G. Barrenechea, V. John, and P. Knobloch, A linearity preserving algebraic flux correction scheme satisfying the discrete maximum principle on general meshes. *Mathematical Models and Methods in Applied Sciences (M3AS)* **27** (2017) 525–548.
- [5] G. Barrenechea, V. John, and P. Knobloch, Analysis of algebraic flux correction schemes. *SIAM J. Numer. Anal.* **54** (2016) 2427–2451.
- [6] G. Barrenechea, V. John, P. Knobloch, and R. Rankin, A unified analysis of algebraic flux correction schemes for convection-diffusion equations. *SeMA* **75** (2018) 655–685.
- [7] P. Bochev, D. Ridzal, M. D’Elia, M. Perego, and K. Peterson, Optimization-based, property-preserving finite element methods for scalar advection equations and their connection to Algebraic Flux Correction. Preprint, 2019, <https://doi.org/10.13140/RG.2.2.20942.72000>.

- [8] T. Chen and C.W. Shu, Entropy stable high order discontinuous Galerkin methods with suitable quadrature rules for hyperbolic conservation laws. *J. Comput. Phys.* **345** (2017) 427–461.
- [9] I. Christov and B. Popov, New non-oscillatory central schemes on unstructured triangulations for hyperbolic systems of conservation laws. *J. Comput. Phys.* **227-11**, (2008) 5736–5757.
- [10] J. Donea, S. Giuliani, H. Laval, and L. Quartapelle, Time-accurate solution of advection-diffusion equations by finite elements. *Comput. Methods Appl. Mech. Engrg.* **193** (1984) 123–145.
- [11] U. Fjordholm, S. Mishra, and E. Tadmor, Energy Preserving and Energy Stable Schemes for the Shallow Water Equations. In F. Cucker, A. Pinkus, and M. Todd (Eds.), *Foundations of Computational Mathematics*, Hong Kong 2008 (London Mathematical Society Lecture Note Series, pp. 93-139). Cambridge: Cambridge University Press, 2009.
- [12] S. Gottlieb, C.-W. Shu, and E. Tadmor, Strong stability-preserving high-order time discretization methods. *SIAM Review* **43** (2001) 89–112.
- [13] J.-L. Guermond and M. Nazarov, A maximum-principle preserving  $C^0$  finite element method for scalar conservation equations. *Computer Methods Appl. Mech. Engrg.* **272** (2014) 198–213.
- [14] J.-L. Guermond, M. Nazarov, B. Popov, and I. Tomas, Second-order invariant domain preserving approximation of the Euler equations using convex limiting. *SIAM J. Sci. Computing* **40** (2018) A3211-A3239.
- [15] J.-L. Guermond, M. Nazarov, B. Popov, and Y. Yang, A second-order maximum principle preserving Lagrange finite element technique for nonlinear scalar conservation equations. *SIAM J. Numer. Anal.* **52** (2014) 2163–2182.
- [16] J.-L. Guermond and B. Popov, Invariant domains and first-order continuous finite element approximation for hyperbolic systems. *SIAM J. Numer. Anal.* **54** (2016) 2466–2489.
- [17] J.-L. Guermond and B. Popov, Invariant domains and second-order continuous finite element approximation for scalar conservation equations. *SIAM J. Numer. Anal.* **55** (2017) 3120–3146.
- [18] A. Kurganov, G. Petrova, and B. Popov, Adaptive semidiscrete central-upwind schemes for non-convex hyperbolic conservation laws. *SIAM J. Sci. Comput.* **29** (2007) 2381–2401.
- [19] D. Kuzmin, Monolithic convex limiting for continuous finite element discretizations of hyperbolic conservation laws. *Comput. Methods Appl. Mech. Engrg.* **361** (2020) 112804.
- [20] D. Kuzmin, Algebraic flux correction I. Scalar conservation laws. In: D. Kuzmin, R. Löhner and S. Turek (eds.) *Flux-Corrected Transport: Principles, Algorithms, and Applications*. Springer, 2nd edition: 145–192 (2012).

- [21] D. Kuzmin, M. Möller, and M. Gurriss, Algebraic flux correction II. Compressible flow problems. In: D. Kuzmin, R. Löhner, S. Turek (eds), *Flux-Corrected Transport: Principles, Algorithms, and Applications*. Springer, 2nd edition, 2012, pp. 193–238.
- [22] D. Kuzmin and M. Quezada de Luna, Subcell flux limiting for high-order Bernstein finite element discretizations of hyperbolic conservation laws. *J. Comput. Phys.* Available online 21 March 2020, 109411, <https://doi.org/10.1016/j.jcp.2020.109411>
- [23] D. Kuzmin and S. Turek, Flux correction tools for finite elements. *J. Comput. Phys.* **175** (2002) 525–558.
- [24] C. Lohmann, *Physics-Compatible Finite Element Methods for Scalar and Tensorial Advection Problems*. Springer Spektrum, 2019.
- [25] R. Löhner, *Applied CFD Techniques: An Introduction Based on Finite Element Methods* (2nd edition). John Wiley & Sons, Chichester, 2008.
- [26] L. Quartapelle, *Numerical Solution of the Incompressible Navier-Stokes Equations*. ISNM **113**, Birkhäuser, Basel, 1993.
- [27] W. Pazner and P.-O. Persson, Analysis and entropy stability of the line-based discontinuous Galerkin method. *J. Scientific Computing* **80** (2019) 376–402.
- [28] H. Ranocha, M. Sayyari, L. Dalcin, M. Parsani, and D.I. Ketcheson, Relaxation Runge-Kutta methods: Fully-discrete explicit entropy-stable schemes for the compressible Euler and Navier-Stokes equations. Preprint [arXiv:1905.09129 \[math.NA\]](https://arxiv.org/abs/1905.09129), 2019.
- [29] D. Ray, P. Chandrashekar, U.S. Fjordholm, and S. Mishra, Entropy stable scheme on two-dimensional unstructured grids for Euler equations. *Commun. Comput. Phys.* **19** (2016) 1111–1140.
- [30] V. Selmin, The node-centred finite volume approach: bridge between finite differences and finite elements. *Comput. Methods Appl. Mech. Engrg.* **102** (1993) 107–138.
- [31] V. Selmin and L. Formaggia, Unified construction of finite element and finite volume discretizations for compressible flows. *Int. J. Numer. Methods Engrg.* **39** (1996) 1–32.
- [32] E. Tadmor, The numerical viscosity of entropy stable schemes for systems of conservation laws I. *Math. Comp.* **49** (1987) 91–103.
- [33] E. Tadmor, Entropy stability theory for difference approximations of nonlinear conservation laws and related time-dependent problems. *Acta Numerica* (2003) 451–512.
- [34] E. Tadmor, Entropy stable schemes. *Handbook of Numerical Analysis, Vol. 17*, Elsevier, 2016.